Please select category below:
Normal Paper ☒
Student Paper ☐
Young Engineer Paper ☐

Propagator for asteroid trajectories tool (PAT2) with educational purposes

Sung Wook Paek [1], Patricia C. Egger [2], Sangtae Kim [3] and Olivier de Weck [4]

[1] *Materials R&D Center, Samsung SDI, Gyeonggi-do 16678, Republic of Korea*
[2] *École Polytechnique Fédérale de Lausanne, Space Engineering Center (eSpace), 1015 Lausanne, Switzerland*
[3] *Center for Electronic Materials, Korea Institute of Science and Technology, Seoul 02792, Republic of Korea*
[4] *Department of Aeronautics and Astronautics, Massachusetts Institute of Technology, Cambridge, MA 02139, United States*

Abstract

Near-Earth asteroids (NEAs) pose potential threats to Earth because their size and trajectory are difficult to predict. Close approaches of small NEAs which may cause local damage have been reported frequently, drawing both public and academic interest. In light of this, a trajectory simulation tool (PAT2) has been developed to predict future NEA positions. Light-weight and open-source, PAT2 is best suited for educators to help students understand the problem of predicting asteroid trajectories. This paper describes the process of developing PAT2 and discusses some case study results.

Keywords: asteroid trajectory, N-body problem, relativistic effects, machine learning, neural network.

Introduction

A potentially hazardous object (PHO) is a near-Earth asteroid or comet whose size and orbit may cause damage to Earth. The Chelyabinsk event (2013) caused 1,500 injuries, exemplifying the level of regional damage from an asteroid as small as 20 meters in diameter. These small asteroids, "city killers," are much more common than extinction-class asteroids whose last impact with Earth was 65 million years ago [1, 2]. An education tool (PAT2; propagator for asteroid trajectory tool) has been developed to help students to learn how to predict the trajectories of dangerous asteroids.

N-body Problem

The N-body problem in astronomical dynamics is chaotic, meaning that small perturbations in initial conditions lead to unpredictable and enormous changes of the system after long-term integration. Equation 1 presents a typical N-body problem amongst celestial bodies, where μ_j is the standard gravitational parameter, the product of the gravitational constant G with the mass of the body m_j. The point mass acceleration is given by the sum of contributions from the other $N-1$ objects, inversely proportional to distance $r_{ij}=|\boldsymbol{r}_j-\boldsymbol{r}_i|=|\boldsymbol{r}_{ij}|$.

$$\ddot{\boldsymbol{r}}_i = \sum_{j\neq i}^{N} \frac{\mu_j(\boldsymbol{r}_j-\boldsymbol{r}_i)}{r_{ij}^3} \tag{1}$$

If relativistic effects are considered, Eqn 1 must be modified to include additional terms derived from a linearized mass tensor [3]. Equation 2 shows these terms containing the speed of light (c) and is called the Einstein–Infeld–Hoffmann equation [4]. Symbols β and γ are parameterized-post-Newtonian parameters whose values are 1 in general relativity [5].

$$\ddot{\boldsymbol{r}}_i = \sum_{j\neq i}^{N} \frac{\mu_j \boldsymbol{r}_{ji}}{r_{ij}^3}\left\{1 - \frac{2(\beta+\gamma)}{c^2}\sum_{k\neq i}\frac{\mu_k}{r_{ik}} - \frac{2\beta-1}{c^2}\sum_{k\neq j}\frac{\mu_k}{r_{jk}} + \gamma\left(\frac{v_i}{c}\right)^2 + (1+\gamma)\left(\frac{v_j}{c}\right)^2 - \frac{2(1+\gamma)}{c^2}\dot{\boldsymbol{r}}_i\cdot\dot{\boldsymbol{r}}_j - \frac{3}{2c^2}\left[\frac{\boldsymbol{r}_{ij}\cdot\dot{\boldsymbol{r}}_j}{r_{ij}^3}\right]^2 + \frac{1}{2c^2}\boldsymbol{r}_{ji}\cdot\ddot{\boldsymbol{r}}_j\right\} + \frac{1}{c^2}\sum_{j\neq i}\frac{\mu_j}{r_{ij}^3}\{\boldsymbol{r}_{ij}\cdot[(2+2\gamma)\dot{\boldsymbol{r}}_i - (1+2\gamma)\dot{\boldsymbol{r}}_j]\}(\dot{\boldsymbol{r}}_i - \dot{\boldsymbol{r}}_j) + \frac{(3+4\gamma)}{2c^2}\sum_{j\neq i}\frac{\mu_j\ddot{\boldsymbol{r}}_j}{r_{ij}} \quad (2)$$

A total of fifteen bodes (N=15) are considered in this study: the Sun, eight planets, Pluto, the Moon, the "Big 3" asteroids (Ceres, Pallas and Vesta) and our asteroid of interest. Only the top three asteroids are considered for simplicity, but increasing the number of main-belt asteroids can help enhance the accuracy and quality of solutions; for example, at least four largest asteroids are needed to precisely simulate the trajectory of Mars.

Methods

Initial Value Problem

The EIH equation needs to be reformulated as an initial value problem (IVP) for numerical integration. Equation 2 is first divided into initial conditions and equations of motion of a state (y) as seen in Eqn 3. The state here is a vector consisting of 90 elements that are velocity and position components of fifteen celestial bodies in Cartesian coordinates. The initial position and velocity data is obtained from the JPL HORIZON website.

$$\begin{cases} y(0) = y_0 \\ y'(t) = f\big(t, y(t)\big) \end{cases} \quad (3)$$

With Eqn 3, the state at any time may be calculated as shown in Eqn 4 where h is the time step. Integration over this time step is subject to numerical errors if the celestial by speeds up or accelerates near the Sun. To achieve higher efficiency and accuracy than Runge-Kutta's methods, many software packages employ multistep methods such as Adams-Bashforth-Moulton (ABM) method to solve ordinary dfferential equations. The higher the ABM order is, the more previous results are used to improve accuracy step. Equation 5 presents the Adams-Bashforth predictor step and the Adams-Moulton corrector step, both with the 5th order [6].

$$y_{n+1} = y(t_n + h) = y(t_n) + \int_{t_n}^{t_n+h} f\big(\tau, y(\tau)\big)d\tau \quad (4)$$

$$\begin{cases} \tilde{y}_{n+1} = y_n + \frac{h}{720}\{1901f(t_n, y_n) - 2774f(t_{n-1}, y_{n-1}) + 2616(t_{n-2}, y_{n-2}) - 1274(t_{n-3}, y_{n-3}) + 251f(t_{n-4}, y_{n-4})\} \\ y_{n+1} = y_n + \frac{h}{720}\{251f(t_{n+1}, \tilde{y}_{n+1}) + 646f(t_n, y_n) - 264f(t_{n-1}, y_{n-1}) + 106f(t_{n-2}, y_{n-2}) - 19f(t_{n-3}, y_{n-3})\} \end{cases} \quad (5)$$

MATLAB Implementation

The above-mentioned IVP was implemented in MATLAB widely used in engineering education. Its built-in function, *ode113*, is a multistep non-stiff ODE solver with variable orders between 1 and 13. A graphic user interface has been implemented to facilitate usage, and the codes may be distributed as executable files or web applications as well.

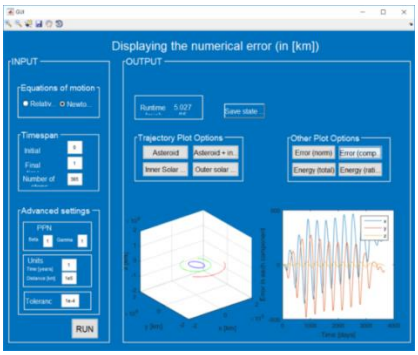

Fig. 1: Graphic user interface of HFOP.

Results

To benchmark HPOF, the following four asteroids were chosen from NASA's Sentry Table which lists potentially hazardous asteroids: Apophis, Icarus, 2007FT3, and 2009VZ39 [7]. Their orbit properties and physical attributes are summarized in Table 1 and Fig 2 [8-10].

Table 1: Physical and orbital properties of asteroids.

Property	Apophis	Icarus	2007 FT3	2009 VZ39
Diameter (m)	370	1440	340	9
Mass (kg)	6.1×10^{10}	1.0×10^{12}	5.5×10^{10}	1.3×10^{6}
Orbital Period (yr)	0.89	1.12	1.2	1.81
Semi-major axis (AU)	0.922	1.078	1.128	1.483
Eccentricity	0.191	0.8369	0.307	0.3824
Inclination (deg)	3.3	22.86	26.83	2.52

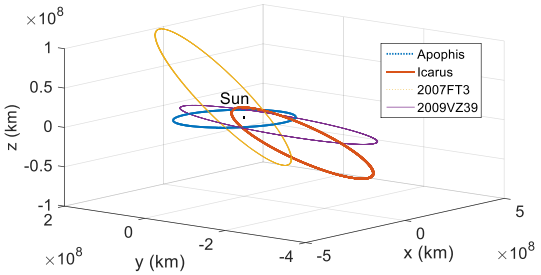

Fig. 2: Orbits of select asteroids in the Solar System.

Apophis

Apophis was once thought to have a high impact probability in 2029 (around 2.7%) when it was first discovered in 2013. Because of its 325-meter diameter, Apophis would survive an atmospheric entry if it were on an Earth-colliding course. Furthermore, it has frequent close approaches with the Earth because they have similar orbit inclination angles relative to the Sun's equator. The minimum orbit intersection distance (MOID) between the two is only 98,652 km, roughly twice fathere from Earth than geostationary satellites.

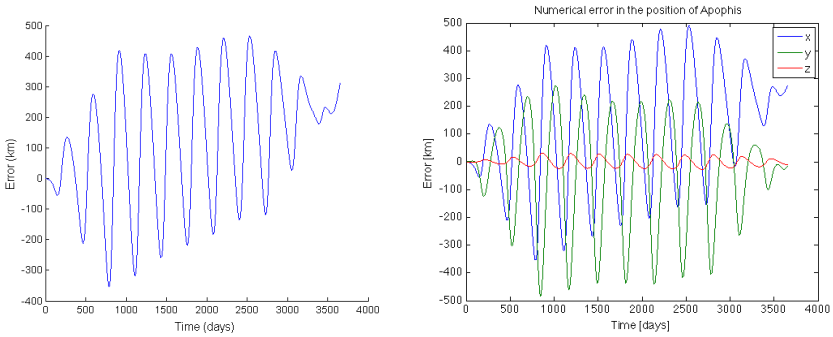

Fig. 3: Errors of Apophis position calculated by HPOF.

The discrepancy between the HFOP solution and the HORIZONS solution is not monotonous but oscillatory as depicted in Fig. 3. The oscillation period is equal to the revolution period of 324 days. Figure 3 (right) illustrates coordinate-wise errors in Apophis' position. The contribution from the *z* component is significantly smaller than *x* and *y* components because the asteroid orbit lies almost in the *xy* plane (ecliptic plane). The maximal error over the 10 year timespan is less than 500 km, satisfying the performance requirement.

Icarus

Icarus has high orbit eccentricity (0.8369) and inclination angle (22.68 degrees), being also the first asteroid observed with radar reflection imaging. The numerical error exceeds the

target value of 1,000 km at peaks, appearing every 408 days which is Icarus' orbital period. Figure 4 shows the *x*, *y* and *z* contributions to the position error. We can observe that the *z*-component is almost the same as the *y*-component, unlike Apophis, because Icarus' orbit is more inclined with respect to the solar equator than Apophis. The locations where the peaks occur correspond to where Icarus is closest to the Sun and moving the fastest. On the other hand, the error is zero when the asteroid is farthest from the Sun and moving the slowest.

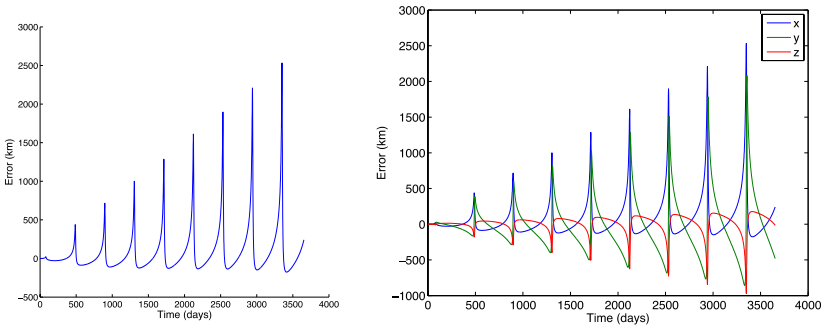

Fig. 4: Errors of Icarus' position calculated by HPOF.

2007 FT3

Asteroid 2007FT3 has the highest orbit inclination angle (26.83 degrees) among four asteroids considered in this study, with its size and mass similar to Apophis. As shown in Fig. 5, the time-series of position errors has combined characteristics of Apophis and Icarus. Like Icarus, 2007FT3 has a large inclination angle and the z component of position errors is no longer negligible; the peaks are smooth whose patterns are similar to Apophis.

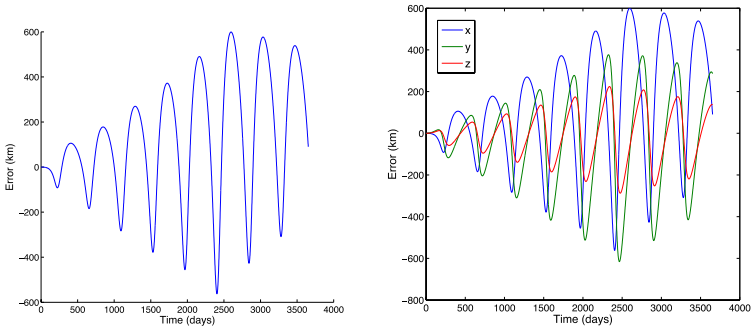

Fig. 5: Errors of 2007FT3' position calculated by HPOF.

2009 VZ39

With a small diameter of 9 m, 2009VZ39 cannot survive the atmospheric entry to reach the Earth surface. Nevertheless, 2009VZ39 is on the NASA Sentry List because of possible damage due to atmospheric explosion. Its position errors exhibit patterns analogous to those of 2007FT3 with larger amplitudes.

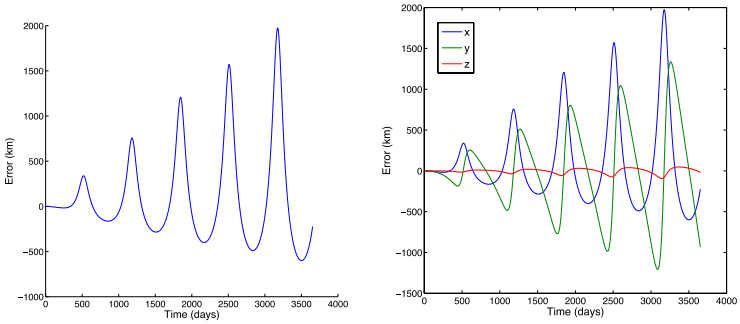

Fig. 6: Errors of 2009VZ39's position calculated by HPOF.

Summary and discussion

Figure 6 presents trade-offs between tolerance and runtime. While the error stops decreasing after certain limits (right), runtime keeps on increasing as tolerance requirement is strengthened (left). Thus optimal tolerance has been identified for each asteroid, as summarized in Table 2. It can be observed that asteroids with high inclination or eccentricity tend to yield more errors or runtime. Since MATLAB is general purpose software, it takes more computation time than tools using Java or FORTRAN. However, PAT2 was written with fewer than 1000 lines of codes, which was made possible by using built-in functions.

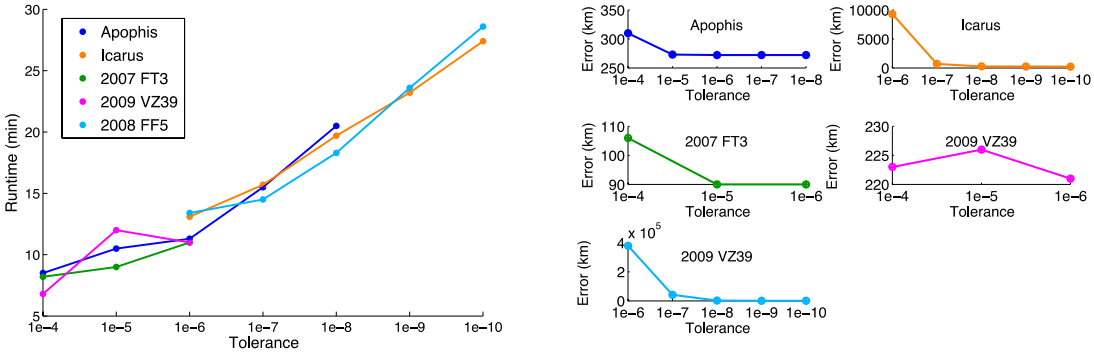

Fig. 6: Runtime and error dependencies with respect to tolerance.

Table 2: Summary of runtime and accuracy of case studies.

Property & Performance	Apophis	Icarus	2007 FT3	2009 VZ39
Eccentricity	0.191	0.8369	0.307	0.3824
Inclination (deg)	3.3	22.86	26.83	2.52
Tolerance ($\log_{10}$)	-6	-9	-5	-4
Max error (km)	489	2500	599	2000
Runtime (min)	11.3	28.5	9	6.8

The periodic patterns of position errors may be exploited, if available, to further calibrate and compensate for compensation (Icarus, 2007FT3, and 2009VZ39). Figure 7 depicts an attempt to predict irregular patterns of Apophis position errors using neural networks [11]. In the figure, the first 300 data points are used for training, based on which time-series predictions are made until the 500th points. Once this feature is fully implemented in PAT2, it may also be possible to use much simpler Newtonian equations rather than EIH equations to boost up the orbit computation speed. The resulting errors can then be corrected with a neural network. Eventually, PAT2 may be useful for teaching machine learning to students as well.

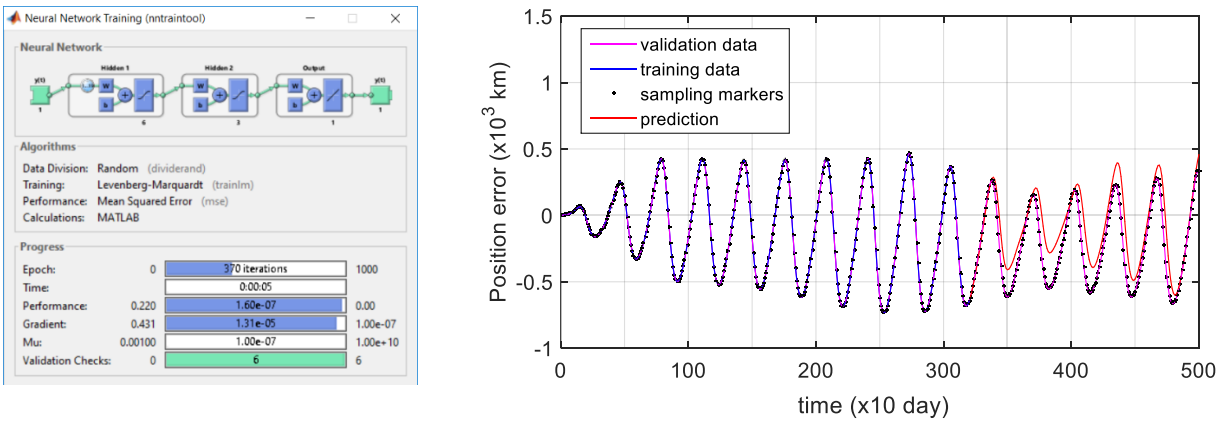

Fig. 7: Prediction of Apophis position errors using MATLAB neural network tool.

Conclusion

A trajectory simulation tool has been developed to predict future positions of near-Earth asteroids (NEA). Named PAT2, this tool is suitable for education purposes owing to its simple implantation. In the follow-up work, the accuracy should be enhanced by incorporating more main-belt asteroids in the model and non-gravitational effects such as solar radiation pressure. Periodic or chaotic errors may also be calibrated using machine learning techniques, helping students to learn the subject matter. Benchmarking PAT2 with NASA's GMAT in asteroid exploration (or deflection) missions would serve as a great case study [12].

References

1. Lal, B. "Defining the Problem", President's Council of Advisors on Science and Technology, Washington D.C., 2016, From *https://obamawhitehouse.archives.gov/sites/*

2. Paek, S. W., Egger, C. P., de Weck, O. L. and Polany, R. "Asteroid deflection campaign design integrating epistemic uncertanities", in *Proceedings of the IEEE Aerospace Conference*, Big Sky, MT, USA, March 5-12, 2016, doi:10.1109/AERO.2016.7500905

3. Brumberg, V. "On derivation of EIH (Einstein-Infeld-Hoffman) equations of motion from the linearized metric of general relativity theory", *Celestial Mechanics & Dynamical Astronomy*, Vol. 99, No. 3, 2007, pp. 245–252, doi:10.1007/s10569-007-9094-5

4. Will, C. M.,"Theoretical frameworks for testing relativistic gravity II: Parameterized post-Newtonian hydrodynamics and the Nordtvedt effect", *Astrophysics Journal*, 163, 1971.

5. Harrison, B. K. and Estabrook, F. B., "Geometric approach to invariance groups and solution of partial differential systems", *Journal of Mathematical Physics*, Vol. 12, 1971.

6. Hairer, E., Nørsett, S. P. and Wanner, G., *Solving ordinary differential equations I: Non-stiff problems* (2nd ed.), Berlin: Springer Verlag, 1993.

7. Chodas, P., "Center for Near Earth Objects Study", URL: https://cneos.jpl.nasa.gov/

8. Chamberlin, A., Yeomans, D., Giorgini, J. and Chodas, P., "Jet Propulsion Laboratory Small-Body Database Search Engine", From *http://ssd.jpl.nasa.gov/sbdb_query.cgi*

9. Paek, S. W. and de Weck, O. L., "A two-stage asteroid deflection campaign consisting of precursor mission and impactor mission", *International Astronautical Congress*, 2014.

10. Paek, S. W., Egger, P. C. and de Weck, O. L., "Rapid prototyping of asteroid deflection campaigns with spatially and temporally distributed phases", *AAS/AIAA Space Flight Mechanics Meeting*, AAS15-333, Williamsburg, VA, USA, January 11-15, 2015.

11. Potocnik, P., "Prediction of chaotic time series with NAR neural network", *Neural Networks course (practical examples)*, 2012.

12. Paek, S.W., de Weck, O. and Kim, S., "A multi-functional paintball cloud for asteroid deflection", Journal of the British Interplanetary Society, Vol. 71, No. 3, pp.81-88, 2018.